Antarctic Science 12 (2): 243–254 (2000) © British Antarctic Survey Printed in the United Kingdom

A study of surface heat fluxes in the Ross Sea (Antarctica)

GIORGIO BUDILLON*, GIANNETTA FUSCO and GIANCARLO SPEZIE

Istituto di Meteorologia e Oceanografia, Istituto Universitario Navale, Via Acton, 38, 80133 Napoli, Italy
**budillon@unina.it*

Abstract: In the polar regions, dynamical and thermodynamical interactions between atmosphere and ocean are strongly influenced by the presence or absence of the ice cover, which forms an insulating layer over the ocean, hindering sensible heat fluxes and forming an effective barrier to evaporation and thus preventing latent heat loss. In the framework of the CLIMA (Climatic Long-term Interactions for the Mass-balance in Antarctica) project of the Italian PNRA (National Program for Antarctic Research) we focused our attention on the evaluation of the heat fluxes between the ocean and the atmosphere in the Ross Sea, where the ice covers the sea for many months of the year. Wherever the ice cover is absent all year round, such as in leads or polynyas, the air-sea fluxes can be very large, especially in winter when the air-sea temperature differences are strong. In this work heat exchanges between sea and atmosphere, whether ice cover was present or not, were calculated from climatological data obtained from the European Centre for Medium Range Weather Forecasts, while sea ice data were collected from the US National Ice Center and National Climatic Data Center. Each of the terms in the sea surface heat budget were computed for 1994 with a temporal resolution of six hours and a spatial resolution of 0.5° using bulk formulae and obtaining monthly averaged horizontal distributions. The surface heat budget is dominated in November, December, January and February by shortwave radiation, while for the other months the turbulent and conductive heat fluxes dominate the heat exchange between the atmosphere and the sea surface. The annual total heat loss at the surface in 1994 has been estimated at about -90 W m^{-2} with the highest heat loss occurring close to the coast; the maximum heat loss occurred in May (-217 W m^{-2}) while in January the heat gain by the ocean was 196 W m^{-2}. In addition, weekly averaged values over the whole Ross Sea from 1994 to 1997 were calculated with the same parameterisation in order to study the temporal variability in this basin of each individual component and of the total surface heat budget. For this purpose only the data inside the continental shelf of the Ross Sea were considered in calculating the averaged fluxes. The 1994–97 total heat budget ranges from -87 to -107 W m^{-2} with an average of -96 W m^{-2}; this amount of heat loss was supposed to be compensated for by the heat advected by the Circumpolar Deep Water and its transport was estimated at about 2.9 Sv.

Received 12 March 1999, accepted 7 February 2000

Key words: circumpolar deep water, Ross Sea, sea ice, surface heat fluxes

Introduction

Antarctica plays a crucial role in global change. The complex air–ice–sea interactions taking place in this area affect surface, intermediate and deep global ocean circulation. The energy transfer (from and into the atmosphere) and its balance develop over a wide range of temporal scales. Coastal and continental shelf areas, where persistent polynya phenomena occur throughout the year, are characterized by strong heat loss and strong ice formation (Ball 1957, Bromwich & Kurtz 1984, Kurtz & Bromwich 1985).

In this study we calculate the surface heat flux and its spatial and temporal variability over the continental shelf of the Ross Sea. Because of its particular configuration, in the Ross Sea the waters coming from the Antarctic Circumpolar Current are transformed into Antarctic bottom, deep, shelf and surface waters through complex processes of interaction with the atmosphere and with the glacial and sea ice (Jacobs *et al.* 1970, Carmack 1977).

The intensity of the inflow and the outflow and the rate of the water mass conversions are clearly related to the seasonal and interannual fluctuations in surface wind stress and heat flux.

In order to define the seasonal cycle of the thermocline and the preconditioning phase of the water column associated with the dense water formation in the Ross Sea, it is important to know both the temporal and the spatial variability of the surface heat flux. This helps to identify where and when the deep water formation is likely to occur. The study of the temporal and spatial variability of the surface heat flux is also important for modelling studies of basin wide thermohaline circulation.

Inthis paper we first calculate the heat budget over the whole Ross Sea in order to investigate its spatial variability in different seasons of 1994 and we then analyse the seasonal and interannual variability over a period of four years (1994–97).

In the Ross Sea the meteorological parameters are monitored in only a few points along the coast where automatic weather stations are located. Data from these stations can only

inadequately represent the meteorological conditions of the whole basin because of the influence of the cold continent. Therefore, for this first attempt to evaluate the surface heat budget in this region we used the European Centre for Medium Range Weather Forecasts (ECMWF) operational analysis data. Despite the possible systematic errors, these data represent a valuable source of information for the definition of the forcing functions of numerical models used to study climatological and interannual time scales.

The study area

The Ross Sea is an ocean basin on the Antarctic continental shelf whose boundaries are Cape Colbeck at 158°W and Cape Adare at 170°E. Its southern boundary is represented by the edge of the Ross Ice Shelf (RIS) at around 78.5°S. This broad ice cover, which extends over nearly half the continental shelf, is about 250 m thick on its northernmost side.

One important dynamic feature of this sector of Southern Ocean is the Antarctic Circumpolar Current (ACC) which moves west to east around Antarctica and interacts with different water masses along its path. It carries the Circumpolar Deep Water (CDW), the most voluminous water mass of the Southern Ocean that extends down to a depth of about 4000 m.

South of the ACC lie vast areas of sluggish flow, many of which are organised into cyclonic gyres. One of them is located north of the Ross Sea and is referred to as the Ross Gyre. The CDW flows into the Ross Gyre and, on reaching the southern limb of the continental slope mixes isopycnally with the shelf waters of the continental shelf (Locarnini 1994).

On reaching the Antarctic continental shelf the CDW moves upward in the water column and mixes, at the continental shelf break, with the shelf waters, forming deep and bottom waters generically named Antarctic Bottom Waters (AABW). AABW entering the Southern Ocean mixes with deep waters to form new CDW.

The mixing of the CDW with the surface and shelf waters on the shelf of the Ross Sea forms a distinct water mass, the Modified Circumpolar Deep Water (MCDW) or Warm Core (WMCO), characterized by a subsurface potential temperature maximum and a dissolved oxygen minimum (Jacobs *et al.* 1985). The MCDW interacts actively with the cold atmosphere, sea and glacial ice to form shelf waters in the Ross Sea (Jacobs *et al.* 1985, Trumbore *et al.* 1991, Locarnini 1994).

It has to be stressed that CDW is generally separated from the shelf waters by a front, namely the Antarctic Slope Front (ASF), a common oceanographic feature of the Antarctic shelf break (Jacobs 1991). This is topographically controlled and interestingly is related to high biological productivity. It also constitutes a source or sink region of deep ocean heat, salt, nutrients, particulate, sediments and atmospheric gases (Trumbore *et al.* 1991).

The shelf waters in the Ross Sea are formed during winter when the upper layers cool and freeze, thus delivering part of their saline content, which increases the salinity of the subsurface waters (Jacobs *et al.* 1985). Shelf waters generally have temperatures close to the surface freezing point, between -1.95°C and -1.75°C, and display higher salinity values in the western sector than in the eastern one (Locarnini 1994). The high salinity in the western sector could be accounted for by the large size of the ice-free areas (polynya) even during the winter period (Kurtz & Bromwich 1983, 1985). These basins, despite being involved in a large ice formation process, are kept open by the strong winds, which remove the ice as soon as it forms. The rejected brine increases the salinity of the subsurface waters, thus forming the densest waters of the Southern Ocean. These water masses, whose salinity increases with depth from 34.75 to 35.00, are named High Salinity Shelf Waters (HSSW, as analysed by Jacobs *et al.* 1985). The presence of the modified CDW in the subsurface layer of the western sector of the Ross Sea plays an important role in HSSW formation: when the surface waters freeze during the winter, the released brine is added to the subsurface waters which already have relatively high salinity values due to the direct influence of the MCDW (Locarnini 1994).

Part of the HSSW is known to move northward along the western sector of the Ross Sea extending as far as the continental shelf break and takes part in the formation of the AABW. Another branch goes southward and flows under the Ross Ice Shelf giving rise to a different type of water named Deep Ice Shelf Water which is characterized by a temperature lower than the freezing point at the sea surface (Jacobs *et al.* 1970). This water is basically formed by cooling and melting at different depths under the Ross Ice Shelf. DISW are primarily located in the central part of the continental shelf; they also move northward making a further contribution to the formation of the Antarctic bottom water (Jacobs *et al.* 1985).

The Ross Sea is thus a well known site of dense water formation related to the winter surface heat losses. The dense water formation process is likely to be extremely sensitive to the inter-annual variability of the atmospheric forcing, making different amounts of dense water available for the bottom water formation processes and for the ventilation of the deep layers outside the continental shelf break.

This study was carried out in two steps. In the first the spatial and temporal variability of the surface heat fluxes were investigated for 1994 by means of monthly averaged values gridded with a spatial resolution of 0.5° and with a temporal resolution of 6 h. The area investigated in the present work extends from 162°E to 160°W and from 70°–78°S, including the continental shelf of the Ross Sea and its continental slope towards the Pacific Sector of the Southern Ocean.

The area investigated was reduced so that it contains only the whole area of the continental shelf of the Ross Sea, assumed to be the 3.9×10^5 km^2 region between the 1000 m isobath, the coastline and the ice shelf (Jacobs & Comiso 1989). The weekly means were calculated over this domain to analyse the average heat exchanged at the surface for the period 1994–97.

The data set

For this study we used operational analyses from 1994–97 provided by the ECMWF (see ECMWF 1994). Data utilised for the flux computations were mean sea level pressure, total cloud cover, wind speed, air temperature (all of them at the surface) and relative humidity (at 1000 hPa). The analyses have a temporal resolution of 6 h (00h00, 06h00, 12h00, 18h00 UTC) and a spatial resolution of 0.5° x 0.5°. The ECMWF scheme use a sea-ice parameterisation that will produces errors in the surface layer air temperature close to the shelves. Therefore we do not estimated the surface heat fluxes along the RIS.

Sea-ice information was obtained from the National Climatic Data Center (NCDC) in Asheville, North Carolina, USA; the data were digitised from the National Ice Center (NIC) weekly charts prepared by the US Navy/National Oceanic and Atmospheric Administration (NOAA) Joint Ice Center, converted into a digital format prescribed by the World Meteorological Organization and are presented in the international Sea Ice Grid (SIGRID) structure on a 0.25° latitude grid; they include total ice concentration, stage of development (thickness) and form of ice for the complete period of record. The ice concentration was used to identify ice covered areas and so the ice thickness was utilised in the computations of the sea ice albedo and of the fraction of the shortwave radiation which penetrated the ice. In order to homogenise the data set the sea-ice data were linearly interpolated in space and time. Because of the lack of ice information for the period 1995–97, the weekly averaged ice-thickness was obtained from the 1994 data set.

Sea surface temperature (SST) weekly data from the NIC with a resolution of 1°x 1° available on the world wide web (ftp://nic.fb4.noaa.gov/pub/ocean/clim1/oisst; R.W. Reynolds, personal communication 1997) report a constant value of -1.8°C over the area investigated. This value is obviously an underestimation of the true one, at least for the summer months; consequently, it was kept at -1.8°C in our winter computations, whereas a value of -0.8°C was used for the summer, an average based on in situ data (see also Kurtz & Bromwich 1985).

Heat flux parameterization and computation

In the no-ice situation the heat flux at the ocean-atmosphere interface may be expressed as follows:

$$Q_T = Q_S + Q_B + Q_H + Q_E$$

where the radiative part consists of the shortwave radiation flux Q_S and the longwave radiation flux Q_B; the turbulent part includes the sensible heat flux Q_H and the latent heat flux Q_E. In the case of sea ice, the surface heat budget is composed also of heat conducted flux through the ice Q_C, and can thus be expressed as:

$$Q_T = Q_S + Q_B + Q_H + Q_E + Q_C$$

Shortwave radiation flux

The flux of solar radiation may be expressed as (see, for instance, Simonsen & Haugan 1996)

$$Q_S = (1 - \alpha)\, C_c T_r S_a \cos\eta$$

where C_c is a cloud cover correction, T_r is the transmittance of the clear sky atmosphere, S_a is the constant Solar, η is the zenith angle of the Sun which depends on latitude, day of the year and solar time and a is the sea surface albedo for open water taken from Payne's (1972) tables; for young ice the latter is strongly dependent on the thickness $d(m)$ (Maykut 1982):

$$\alpha = 0.08 + 0.44 d^{0.28}$$

The cloud cover correction may be written as:

$$C_c = a_1 - a_2 C^{a_3} + a_4 h$$

where h is the solar elevation at noon in degrees and C is the fractional cloud cover. Different values for the empirical constants ($a_{1\text{-}4}$) may be found in literature. In Table I we consider the cloud cover corrections by Laevastu (1960) and Reed (1977).

We opted for the Laevastu formula because it has been applied in polar studies for sea-ice modelling (Parkinson & Washington 1979) and computations of the heat fluxes in the Nordic Seas (Hakkinen & Cavalieri 1989). Conversely, the Reed (1977) formula is based on observations from the tropics to the Alaskan Gulf and gives a random error estimated about ± 20% (Reed 1977).

The simplest expression for the clear sky transmittance is a constant value (T_r = 0.7) as applied by Bunker (1976) and Isemer *et al.* (1989). However, at high latitudes the effect of the larger distance through the atmosphere that the sunlight has to penetrate becomes significant. Water vapour and other components in the atmosphere may also have non-negligible effects (Simonsen & Haugan 1996). On the basis of model calculations, Shine (1984), modifying a Zillman-type model (Zillman 1972) introduced this formula for polar regions:

$$T_r = \frac{\cos\eta}{\beta_1 \cos\eta + (\beta_2 + \cos\eta)\, e(T_a)\beta_3 + \beta_4}$$

where the constants are: $\beta_1 = 1.0$, $\beta_2 = 1.0$, $\beta_3 = 10^{-5}$, $\beta_4 = 0.046$.

This formula was used for the Antarctic (Heil *et al.* 1996) and the Arctic Mediterranean (Simonsen & Haugan 1996).

The water vapour pressure $e(T_a)$ at the air temperature T_a was calculated from the relative humidity and from the

Table I. Empirical constants in the cloud cover corrections.

	a_1	a_2	a_3	a_4
Laevastu (1960)	1	0.6	3	0
Reed (1977)	1	0.62	1	0.0019

saturation vapour pressure e_s (in hPa), which depends only on T_a (K), and is derived from an empirical relationship

$$e_s = 6.11\ 10^{(A\,T)/(B+T)}$$

where (A, B) = (7.5, 35.86) for open water and (9.5, 7.66) over ice (Parkinson & Washington 1979).

In the presence of the ice cover, the shortwave radiation is used in the computation of I_0, which is the fraction of Q_S that penetrates the ice, depending on the ice thickness (Maykut 1982).

$$I_0 = 0.805\ Q_S \exp(-1.5d + 0.15)$$

The penetration of radiation occurs only when the ice is snow-free, as is assumed in the present work.

Net longwave radiation flux

The net longwave radiation flux is calculated from the Berliand & Berliand (1952) formula using Budyko's (1974) cloud cover correction. Its expression is

$$Q_B = 4\varepsilon\sigma T_A^3\left(T_A - T_{Sfc}\right) + \varepsilon\sigma T_A^4\left(0.39 - 0.05\sqrt{e_A}\right)\left(1 - \chi C^2\right)$$

where e = ocean emissivity, σ = Stefan-Boltzmann constant, C = cloud cover, e_A = atmospheric vapour pressure (hPa), T_A = air temperature (K), T_{Sfc} = surface temperature of the ocean or ice (K), χ = varies linearly with latitude from 0.5 at the equator to 1.0 at the pole.

The ice temperature, which is normally higher than the air temperature but lower than the water temperature underneath the ice, was estimated using the following empirical formula:

$$T_{Ice} = T_A + f\,(T_w - T_A)$$

where T_w is water temperature (271.16 K) and f is a parameter empirically determined from the observed brightness temperature.

Sensible heat flux

The sensible heat flux represents the heat gained or lost at the sea surface by the processes of conduction and convection, as defined by the bulk formula:

$$Q_H = \rho_A C_p C_H |\overline{V}|\left(T_A - T_{Sfc}\right)$$

where ρ_A = density of moist air (kg m^{-3}), C_p = specific heat capacity, C_H = turbulent exchange coefficient, T_{Sfc} = surface temperature of the ocean or ice (K), T_A = air temperature (K), $|\overline{V}|$ = wind speed (m s^{-1}).

Latent heat flux

The heat flux from the sea to the atmosphere via evaporation is usually the most important flux in regions of deep ocean convection and is defined by the bulk formula:

$$Q_E = \rho_A L_E C_E |\overline{V}|\left(q_A - q_S\right)$$

where: ρ_A = density of moist air (kg m^{-3}), L_E = latent heat of vaporization or of sublimation (in the case of ice), C_E = turbulent exchange coefficient, q_S = saturation specific humidity of air with temperature T_{Sfc}, q_A = specific humidity of the air, $|\overline{V}|$ = wind speed (m s^{-1}).

The heat exchange coefficients depend on wind speed and atmospheric stability, but the choice of these coefficients is not trivial. The simplest approach is to assume a constant coefficient, but an appropriate value for the area of interest is not easy to find in literature. On the basis of experience of sea ice modelling results and polar observations, Maykut (1978, 1982) found that an appropriate value is 1.75×10^{-3}; this value was used for the estimation of the turbulent terms in the present work and falls within the range of reported values in literature, which vary from 1.1×10^{-3} (Large & Pond 1982) to $(2.0–2.5) \times 10^{-3}$ (Maykut 1978, Hakkinen & Cavalieri 1989).

Conductive heat flux

The conductive heat flux Q_C through the snow-free ice is given by (Semtner 1976):

$$Q_C = (K_I / d)(T_{Sfc} - T_B)$$

where K_I is the thermal conductivity of the ice and has a value of 2.04 Wm^{-1}K^{-1} while T_B is the temperature at the bottom of the ice, assumed to coincide with the freezing point of seawater.

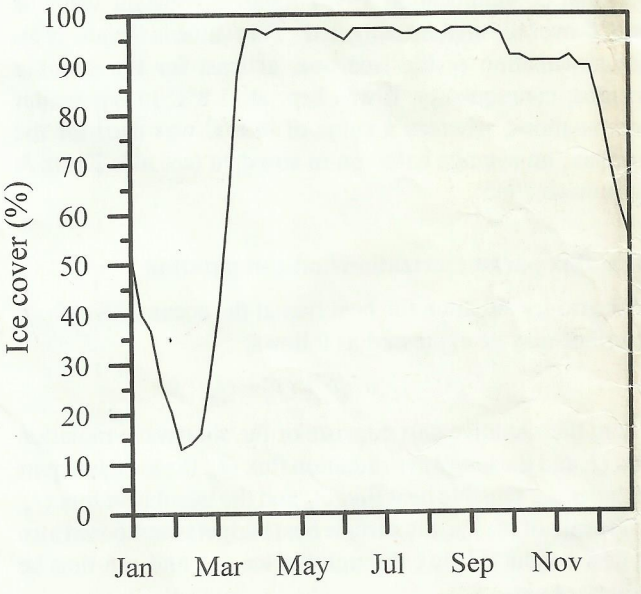

Fig. 1. Ice cover percentage computed in the Ross Sea in 1994 from the NIC and NCDC data-set.

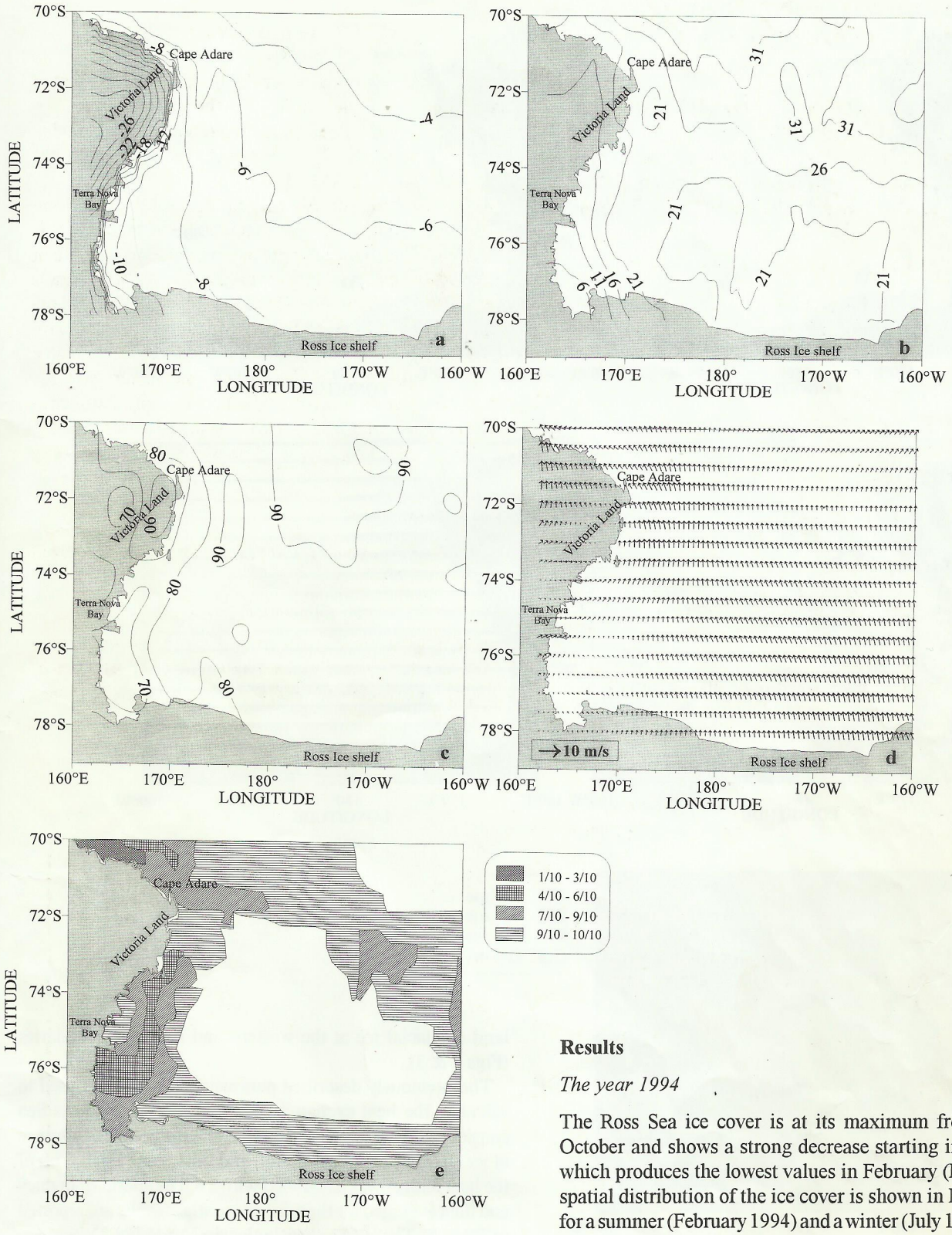

Fig. 2. Monthly means for February 1994 of **a**. air temperature (°C), **b**. total cloud cover (%), **c**. relative humidity (%), **d**. wind speed (m s^{-1}), **e**. ice cover (tenths).

Results

The year 1994

The Ross Sea ice cover is at its maximum from April to October and shows a strong decrease starting in November which produces the lowest values in February (Fig. 1). The spatial distribution of the ice cover is shown in Figs 2e & 3e for a summer (February 1994) and a winter (July 1994) month. In February a region of high ice cover is generally found in the western sector, probably due to wind forcing, characterized by a cyclonic direction, and by the consequent ocean surface circulation. Meteorological parameters show a characteristic gradient in a SW–NE direction induced by the presence of the

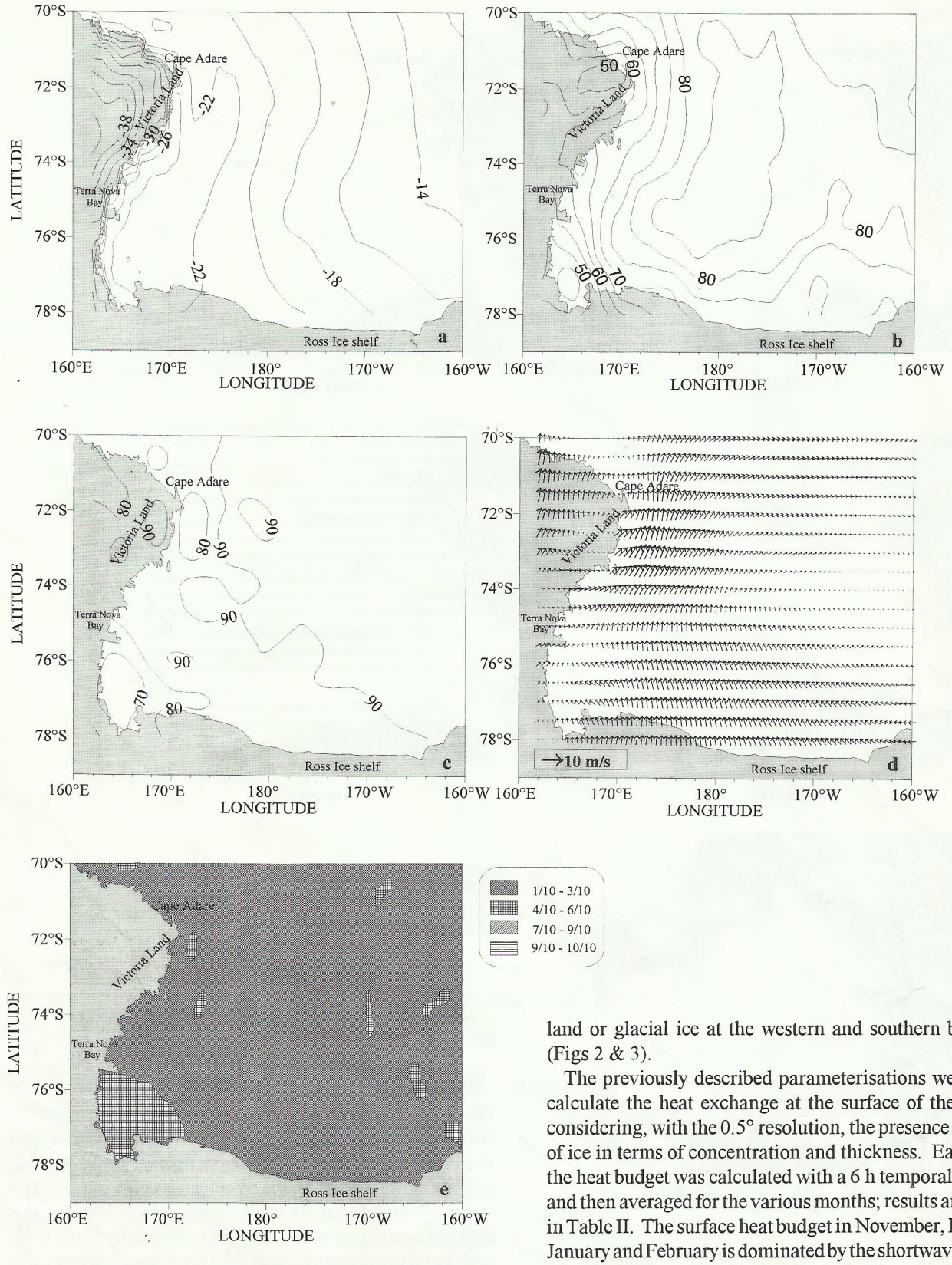

Fig. 3. Monthly means for July 1994 of **a**. air temperature (°C), **b**. total cloud cover (%), **c**. relative humidity (%), **d**. wind speed (m s^{-1}), **e**. ice cover (tenths).

land or glacial ice at the western and southern boundaries (Figs 2 & 3).

The previously described parameterisations were used to calculate the heat exchange at the surface of the Ross Sea considering, with the 0.5° resolution, the presence or absence of ice in terms of concentration and thickness. Each term of the heat budget was calculated with a 6 h temporal frequency and then averaged for the various months; results are reported in Table II. The surface heat budget in November, December, January and February is dominated by the shortwave radiation and then becomes positive, while during the other months the turbulent and conductive heat fluxes dominate the heat exchange between the atmosphere and the sea surface.

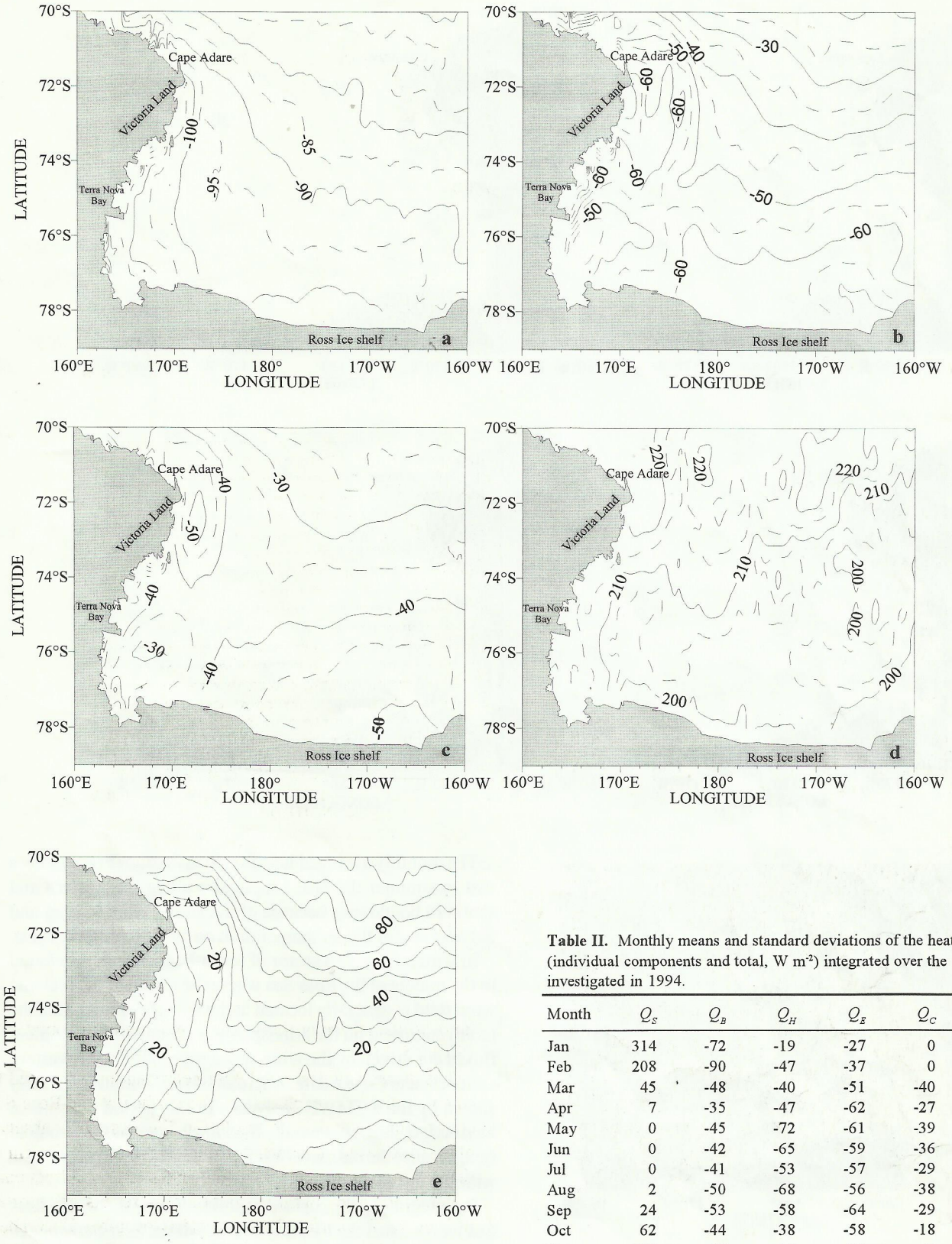

Fig. 4. Monthly means for February 1994 of **a**. longwave radiation flux (W m^{-2}), **b**. sensible heat flux (W m^{-2}), **c**. latent heat flux (W m^{-2}), **d**. shortwave radiation flux (W m^{-2}), **e**. surface heat flux (W m^{-2}).

Table II. Monthly means and standard deviations of the heat flux (individual components and total, W m^{-2}) integrated over the area investigated in 1994.

Month	Q_S	Q_B	Q_H	Q_E	Q_C	Q_T
Jan	314	-72	-19	-27	0	196
Feb	208	-90	-47	-37	0	34
Mar	45	-48	-40	-51	-40	-134
Apr	7	-35	-47	-62	-27	-164
May	0	-45	-72	-61	-39	-217
Jun	0	-42	-65	-59	-36	-202
Jul	0	-41	-53	-57	-29	-180
Aug	2	-50	-68	-56	-38	-210
Sep	24	-53	-58	-64	-29	-180
Oct	62	-44	-38	-58	-18	-96
Nov	125	-47	-13	-38	-7	20
Dec	171	-49	-3	-28	-2	89
Mean	80	-51	-44	-50	-22	-87
s d	103	15	22	13	16	137

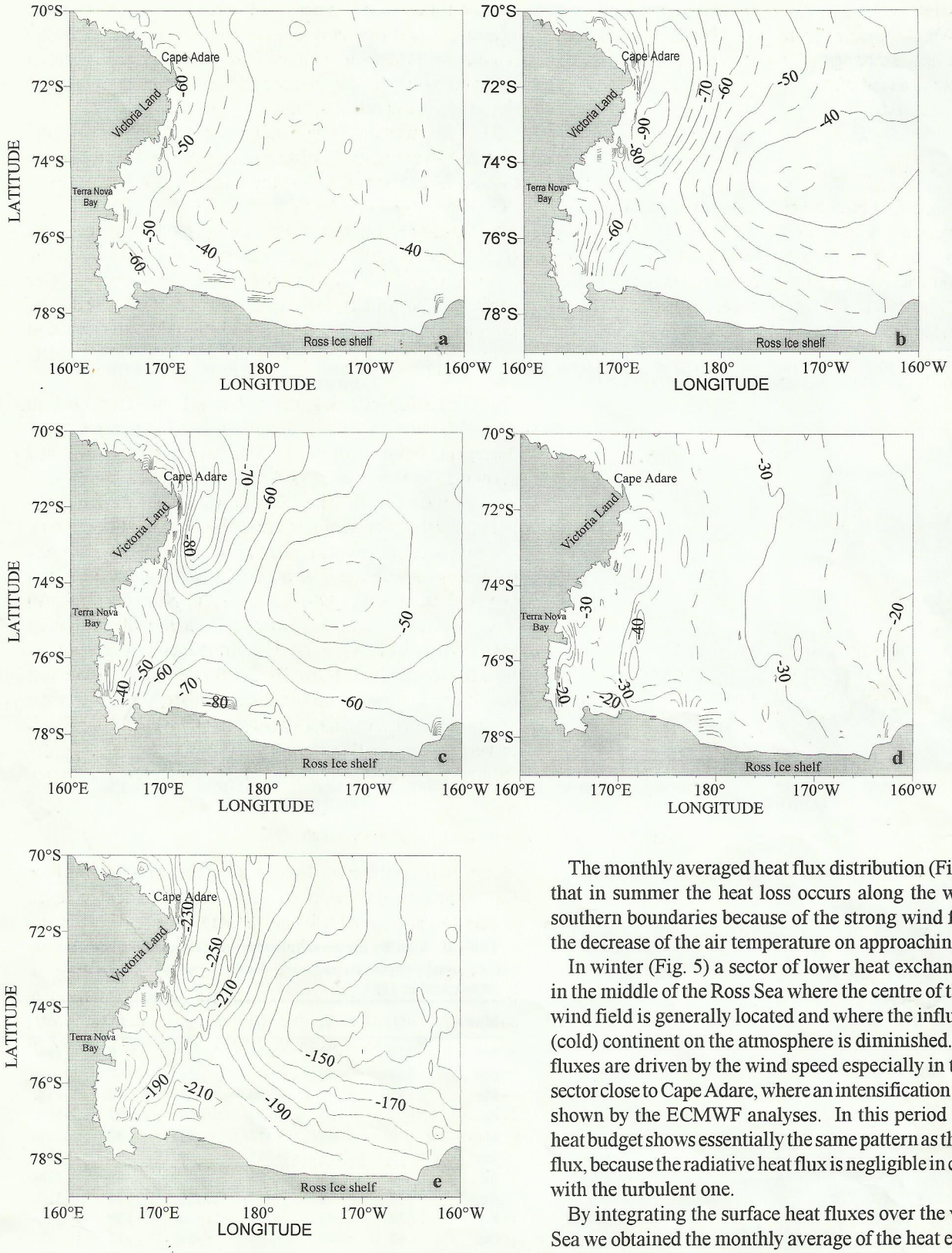

Fig. 5. Monthly means for July 1994 of **a**. longwave radiation flux (W m^{-2}), **b**. sensible heat flux (W m^{-2}), **c**. latent heat flux (W m^{-2}), **d**. conductive heat flux (W m^{-2}), **e**. surface heat flux (W m^{-2}).

The monthly averaged heat flux distribution (Fig. 4) shows that in summer the heat loss occurs along the western and southern boundaries because of the strong wind forcing and the decrease of the air temperature on approaching the coast.

In winter (Fig. 5) a sector of lower heat exchange is found in the middle of the Ross Sea where the centre of the cyclonic wind field is generally located and where the influence of the (cold) continent on the atmosphere is diminished. Turbulent fluxes are driven by the wind speed especially in the western sector close to Cape Adare, where an intensification is generally shown by the ECMWF analyses. In this period the surface heat budget shows essentially the same pattern as the turbulent flux, because the radiative heat flux is negligible in comparison with the turbulent one.

By integrating the surface heat fluxes over the whole Ross Sea we obtained the monthly average of the heat exchange in this region (Fig. 6a). In 1994 heat exchange was positive (i.e. heat was absorbed by the sea) only between November and February while for the remaining period it was always negative. The maximum heat loss occurred in May with a value of about

-220 W m^{-2}, while in January the computed maximum heat gain was 196 W m^{-2}. As expected, the annual mean distribution of the surface heat exchange (Fig. 6b) was negative, with a typical gradient directed offshore; heat loss decreased as the coast was approached.

1994–97 interannual variability

Figure 7 shows the results obtained by estimating from the 6 h ECMWF operational analyses the weekly averaged surface heat fluxes for the whole Ross Sea continental shelf from 1994 –97. Moreover, for each term of the total budget yearly means have been estimated and are reported in Table III. The yearly budget ranges from -87 to -102 W m^{-2} with an average value of -96 W m^{-2}.

Figure 7 reveals that important variations in the surface heat budget of the Ross Sea occurred in the period investigated. The most significant inter-annual fluctuation is shown by the maximum of the solar radiation (Fig. 7a) at the surface caused by cloud cover, the only parameter varying interannually for the shortwave parameterisation.

The long wave radiation ranges from -110 to -40 W m^{-2} (Fig. 7b) showing the lowest values generally during the first months of the years; the mean value for the four years is -55 W m^{-2} with a s d of 4 W m^{-2}.

Of particular interest is the abrupt change of heat loss (Fig.7c) by sensible heat at each end of February when the meteorological forcing switches from summer to winter conditions (particularly in the wind stress) and the ice insulating layer has not yet developed. In this graph values are near zero in the summer months. The annual mean is -45 W m^{-2} and its s d is 3 W m^{-2}.

The latent heat component is probably the most regular term (Fig. 7d) showing the lowest values, as expected, generally during the summer season; the mean value for the investigated period is -50 W m^{-2} with a s d of 2 W m^{-2}.

The conductive flux has a mean value of -20 W m^{-2} and represents the least significant contribution to the total budget.

Previous estimates of monthly averaged surface heat fluxes in the Ross Sea were carried out by Kurtz & Bromwich (1985) and by Van Woert (1999) for the Terra Nova Bay polynya area. These data cannot easily be compared with our results because they were obtained for a limited coastal area of the Ross Sea that is characterized by peculiar local meteorological conditions. Our heat surface estimates are lower than their results; from a limited data set (in time and space) it is difficult to verify whether this discrepancy is due to any specific temporal or spatial characteristics of the situation considered.

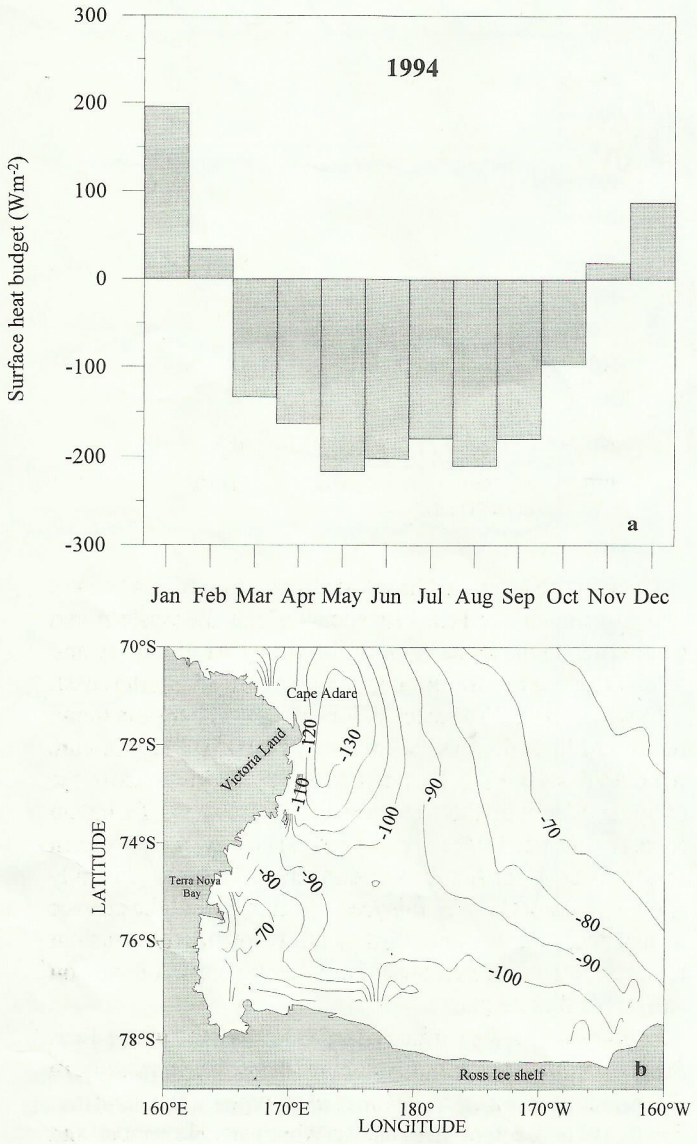

Fig. 6. Annual mean of the surface heat budget for the 1994 **a**. integral over the studied area, **b**. horizontal distribution.

Sensitivity and error analysis

There are several factors that can affect the validity of the heat flux estimates, including errors in the basic observations, uncertainties in the bulk formulae themselves and inadequate sampling. The ECMWF data, being a model generated data set, have the significant advantage of a complete coverage in time and space which reduces the problem of inadequate sampling. Nevertheless, this data set has systematic errors, which can be hard to estimate. Some studies (Trenberth &

Table III. Annual means and standard deviations of the heat flux (individual components and total, W m^{-2}) integrated over the continental shelf of the Ross Sea for the period 1994–97.

	Q_S	Q_B	Q_H	Q_E	Q_C	Q_T
1994	80	-58	-47	-48	-23	-96
1995	78	-59	-48	-50	-23	-102
1996	76	-53	-41	-49	-19	-87
1997	67	-49	-44	-54	-20	-99
Mean	75	-55	-45	-50	-21	-96
s d	5	4	3	2	2	6

Olson 1988, Genthon & Braun 1995, Cullather & Bromwich 1997) have evaluated the analyses produced by the ECMWF comparing them with raw insonde, ship and automatic weather station (AWS) information and with data sets from other archives. These studies show a preference for the ECMWF analyses for atmospheric investigation in the Southern Hemisphere. A careful study on the validation of the ECMWF operational analyses in Antarctica has been performed by Cullather & Bromwich (1997). In the present work a comparison of ECMWF analyses with pressure measurements from AWS units of US Antarctic Program reveals a good agreement for the 10-year period from 1985–94. Moreover a comparison of the near-surface temperature and wind fields with synthesized long-duration studies also show the ECMWF to be more realistic than the National Centers for Environmental Prediction (NCEP) analyses. In the same study, further comparisons of pressure, temperature, relative humidity and wind fields using ship data from the RV *Nathaniel B. Palmer* reveal the ECMWF to be in substantial agreement with the observational data.

We performed a sensitivity analysis of the surface heat fluxes Q_B, Q_H, Q_E and Q_C to the different meteorological inputs in order to study the possible influence of errors in our results.

The following procedure was adopted in order to estimate the range of variability on fluxes Q_B, Q_H, Q_E and Q_C. First, monthly averages (M) and standard deviations (s d) were computed for each grid point of the parameter fields used in the calculations, namely, total cloud cover, mean sea level pressure, air temperature, relative humidity and wind speed. Let Q be the basin-averaged heat fluxes computed by means of the fields for all the parameters. Then, the heat fluxes were computed using the fields M + s d and M - s d for one selected parameter and the average fields m for the others, obtained Q_+ and Q_- respectively. An evaluation of the range of variability on the heat fluxes attributed to the variability on the selected parameter was given by the quantity $k = (|Q-Q_+| + |Q-Q_-|)/2$. This procedure was then repeated for each parameter and the values of k so obtained were combined quadratically to estimate the overall range of variability.

Table IV. Monthly mean values and range of variability in 1994 for the longwave, turbulent and conductivity terms. All units are in W m^{-2}.

Month	Q_B	Q_H	Q_E	Q_C
Jan 94	-72 ± 8	-19 ± 13	-27 ± 9	0
Feb 94	-90 ± 7	-47 ± 22	-37 ± 12	0
Mar 94	-48 ± 15	-40 ± 14	-51 ± 14	-40 ± 6
Apr 94	-35 ± 14	-47 ± 15	-62 ± 15	-27 ± 3
May 94	-45 ± 14	-72 ± 19	-61 ± 13	-39 ± 3
Jun 94	-42 ± 14	-65 ± 16	-59 ± 13	-36 ± 3
Jul 94	-41 ± 15	-53 ± 17	-57 ± 14	-29 ± 4
Aug 94	-50 ± 13	-68 ± 16	-56 ± 11	-38 ± 3
Sep 94	-53 ± 12	-58 ± 17	-64 ± 15	-29 ± 3
Oct 94	-44 ± 15	-38 ± 12	-58 ± 15	-18 ± 3
Nov 94	-47 ± 14	-13 ± 7	-38 ± 13	-7 ± 3
Dec 94	-49 ± 13	-3 ± 4	-28 ± 11	-2 ± 3

Table IV gives the results for the longwave heat flux as a function of total cloud cover, air sea temperature difference, mean sea level pressure and relative humidity, for the sensible and latent heat flux as a function of wind speed and air–sea temperature difference assuming that the SST variability is equal zero, for the conductive flux as a function of the surface–bottom ice temperature difference assuming that the bottom ice temperature error is equal to zero.

As expected, the range of variability for the turbulent heat fluxes is greater during the winter period than in summer because of the strong dependence of these terms on the wind speed. The anomalous value for February 1994 in Q_H is due to high values of the air temperature in this period. During the

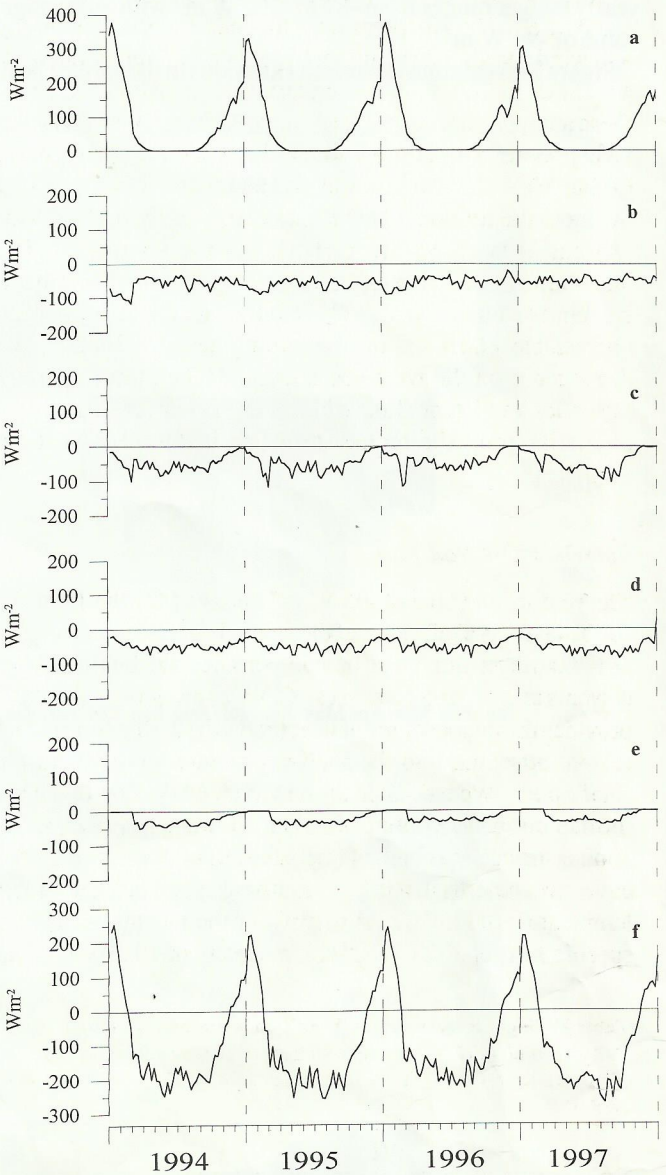

Fig. 7. Time series of surface weekly averaged heat fluxes for the period 1994–97. **a**. Time series of Q_S (W m^{-2}), **b**. time series of Q_B (W m^{-2}), **c**. time series of Q_H (W m^{-2}), **d**. time series of Q_E (W m^{-2}), **e**. time series of Q_C (W m^{-2}), **f**. time series of Q_T (W m^{-2}).

summer, when the longwave radiation is dominant, the range of variability of the Q_B is small and it is primarily dependent on the air temperature; while during the winter the large variability is due to cloud cover changes. The conductivity term displays its maximum range of variability at the end of the summer when the freezing processes of the surface layers start; it remains constant during all the following months.

Moreover, using the results of the statistical study performed by Cullather & Bromwich (1997), particularly the calculated standard error between the *in situ* measurements and the ECMWF analyses, we obtained an estimate of the propagation error in the bulk formulae used in our work. We applied the previously described procedure using the ECMWF summer averaged parameters and the Cullather & Bromwich (1997) standard deviation for pressure, temperature, relative humidity and wind speed. The results are reported in Table V and give a measure of the possible uncertainty of our estimates. From these analyses, during summer, uncertainties in the mean sea level pressure do not show any noticeable effect on Q_B or Q_E (Table V). The influence of the air temperature is strong owing to the turbulent heat fluxes (39% for Q_H and 14% for Q_E) and it is of the order of 5% for the longwave. The uncertainties in the relative humidity are found to have a perceptible effect on the Q_E (6%) although they have no appreciable effect on the remaining terms. Finally, the dependence on the wind speed errors is the most important factor for the latent flux, while it is, as expected, not very dissimilar from the temperature one in the sensible term estimates.

Inferred CDW transport

The year mean value of -96 W m^{-2} obtained for the 1994–97 can be taken as a reference of the yearly heat loss in this region at the surface; this must be compensated for by deep-level currents and mixing processes. CDW coming from the ACC provides the major source of heat (and salt) in this continental region, intruding into the shelf region and mixing with the shelf waters. We estimated the necessary CDW flow that must intrude on to the continental shelf in order to preserve the annual surface heat budget (considering in this case only the advective heat transport). Assuming a mean shelf water temperature of -1.6°C and +1.5°C for the incoming CDW, a specific heat of 3978 J Kg^{-1} K^{-1}, a density of 1028 Kg m^{-3} an average transport of about 2.9 Sv (1 Sv = 10^6 m^3 s^{-1}) was found. Similar transport values are found for the remaining 1995–97 period (Table VI). These values represent a significant fraction of the total baroclinic transport (8.5 Sv; Gouretski 1999) of the Ross Gyre that drives the clockwise circulation patterns outside the continental shelf of the Ross Sea carried by the CDW along the shelf break.

Table V. Summer mean values (W m^{-2}) and error estimates using Cullather *et al.* (1997) standard deviation for mean sea level pressure (ErrP), air temperature (ErrT), relative humidity (ErrRh) and wind speed (ErrV).

	Q_B	Q_H	Q_E
Summer mean	-70	-23	-31
ErrP	0%	-	0%
ErrT	5%	39%	14%
ErrRh	1%	0%	6%
ErrV	-	64%	49%

Conclusions

The results obtained for the surface heat fluxes from the ECMWF analyses obviously require validation. The estimates relative to the surface heat budget appear lower than the known values estimated for different years and only for a coastal area in the western Ross Sea using *in situ* meteorological data set. On the basis of only four years of climatology observations it is difficult to verify if this discrepancy is due to a systematic error in the data or to specific characteristics of the period considered and a more exhaustive answer can only be obtained from an extension in time of the heat flux computations. In particular a more detailed check on the cloud and ice cover is crucial for more realistic results. In addition, a different parameterisation for the conductive term can be used to verify its role in the total budget.

The computed heat fluxes show extremely strong spatial and temporal variability in the Ross Sea. The largest heat losses can occur during the months of May–August, while during the period November–February the heat budget becomes positive. A sector where the turbulent terms dominate the total surface heat fluxes, producing a strong negative budget, was found close to Cape Adare in the north-western Ross Sea, which is probably related to a recurrent region of strong wind stress.

Our results did not show any significant interannual variability in the surface heat budget when we estimated the year averaged values during the four years considered: during the period investigated (1994–97) the total budget shows a mean value of -96 W m^{-2} with a s d of 6 W m^{-2}.

The estimation of CDW transport entering the continental shelf of the Ross Sea, based on heat budget considerations, gives a mean value of 2.9 Sv (s d = 0.2) which represents a significant fraction of the westward flow of the southern limb of the Ross Gyre. Of course, this estimation represents an upper limit to the real value because it is obtained by considering

Table VI. Annual means and standard deviations of the total heat flux (W m^{-2}) for the period 1994–97 and related CDW transport (Sv).

	Q_t	F_{cdw}
1994	-96	2.9
1995	-102	3.1
1996	-87	2.7
1997	-99	3
Mean	-96	2.9
s d	6	0.2

only advective transport (neglecting diffusive transport) performed by the CDW to balance the total heat loss at the surface.

An extension of the period of investigation and numerical experiments using the general circulation model of the Ross Sea forced with the surface heat fluxes examined in this paper will provide more information about the role of the forcing functions in dense water mass formation.

Acknowledgements

This study was performed as part of the Italian "National Program for Antarctic Research" and was financially supported by ENEA through a joint research program. The operational analyses data were supplied by ECMWF. We would like to thank the Italian Meteorological Service and, particularly, Colonel G. Tarantino and Major C. Gambuzza for their invaluable technical assistance. We also thank the referees for their helpful comments.

References

Ball, F.K. 1957. The katabatic winds of Adélie Land and King George V Land. *Tellus*, **9**, 201–208.

Berliand, M. & Berliand, T. 1952. Determining the net longwave radiation of the Earth with consideration of the effect of cloudiness. *Izvestia Akademii Nauk SSSR Seriya Geofizika*, **1**, 1–63.

Bromwich, D.H. & Kurtz, D.D. 1984. Katabatic wind forcing of the Terra Nova Bay polynya. *Journal of Geophysical Research*, **89**, 3561–3572.

Budyko, M.I. 1974. Climate and life. San Diego:Academic Press, 508 pp.

Bunker, A.F. 1976. Computations of surface energy flux and annual air–sea interaction cycles of the North Atlantic Ocean. *Monthly Weather Review*, **104**, 1122–1140.

Carmack, E.C. 1977. Water characteristics of the Southern Ocean South of the Polar Front. *In* Angel, M. & Deacon, G., *eds. A Voyage of discovery: 70th Anniversary Volume. Supplement to Deep Sea Research.* New York: Pergamon Press, 15–42.

Cullather, R.I. & Bromwich, D.H. 1997. Validation of operational numerical analyses in Antarctic latitudes. *Journal of Geophysical Research*,**102** (D12), 13761–13784.

ECMWF 1994. The description of the ECMWF/WCRP level III - A global atmospheric data archive. ECMWF Technical Report, 210 pp. [Unpublished].

Genthon, C. & Braun, A. 1995. ECMWF analyses and predictions of the surface climate of Greenland and Antarctica. *Journal of Climate*, **8**, 2324–2332.

Gouretski, V. 1999. The large-scale thermohaline structure of the Ross Gyre. *In* Spezie, G. & Manzella, G.M.R., *eds. Oceanography of the Ross Sea, Antarctica.* Milan: Springer-Verlag Italia, 77–100.

Hakkinen, S. & Cavalieri, D.J. 1989. A study of oceanic surface heat fluxes in the Greenland, Norwegian and Barents seas. *Journal of Geophysical Research*, **94**, 6145–6157.

Heil, P., Allison, I. & Lytle, V.I. 1996. Seasonal and interannual variations of the oceanic heat flux under a landfast Antarctic sea ice cover. *Journal of Geophysical Research*, **101**(C11), 25 741–25 752.

Isemer, H.J., Willbrand, J. & Haase, L. 1989. Fine adjustment of large-scale air–sea energy flux parameterizations by direct estimates of ocean heat transport. *Journal of Climate*, **2**, 1173–1184.

Jacobs, S.S. 1991. On the nature and significance of the Antarctic Slope Front. *Marine Chemistry*, **35**, 9–24.

Jacobs, S.S. & Comiso, J.C. 1989. Sea ice and oceanic processes on the Ross Sea continental shelf. *Journal of Geophysical Research*, **94**(C12), 18 195–18 211.

Jacobs, S.S., Amos, A.F. & Bruchhausen, P.M. 1970. Ross Sea oceanography and Antarctic bottom water formation. *Deep-Sea Research*, **17**, 935–962.

Jacobs, S.S., Fairbanks, R.G. & Horibe, Y. 1985. Origin and evolution of water masses near the Antarctic continental margin: evidence from $H_2{}^{18}O/H_2{}^{16}O$ ratios in seawater. *Antarctic Research Series*, **43**, 59–85.

Kurtz, D.D. & Bromwich, D.H. 1983. Satellite observed behaviour of the Terra Nova Bay polynya. *Journal of Geophysical Research*, **88**, 9717–9722.

Kurtz, D.D. & Bromwich, D.H. 1985. A recurring atmospherically-forced polynya in Terra Nova Bay. *Antarctic Research Series*, **43**, 177–201.

Laevastu, T. 1960. Factors affecting the temperature of the surface layer of the sea. *Commentationes Physico-Mathematicae*, **25**(1), 8–134.

Large, W.G. & Pond, S. 1982. Sensible and latent heat flux measurements over the ocean. *Journal of Physical Oceanography*, **12**, 464–482.

Locarnini, R.A. 1994. *Water masses and circulation in the Ross Gyre and environs.* PhD. dissertation. Texas A&M University, 87 pp. [Unpublished]

Maykut, G.A. 1978. Energy exchange over young sea ice in the central Arctic. *Journal of Geophysical Research*, **83**, 3646–3658.

Maykut, G.A. 1982. Large-scale heat exchange and ice production in the central Arctic. *Journal of Geophysical Research*, **87**, 7971–7984.

Payne, R.E. 1972. Albedo of the sea surface. *Journal of Atmospheric Science*, **29**, 959–970.

Parkinson, C.L. & Washington, W.M. 1979. A large-scale numerical model of the sea ice. *Journal of Geophysical Research*, **84**, 311–337.

Reed, R.K. 1977. On estimating insolation over the ocean. *Journal of Physical Oceanography*, **7**, 482–485.

Semtner Jr, A.J. 1976. A model for the thermodynamic growth of sea ice in numerical investigations of climate. *Journal of Geophysical Research*, **6**, 379–389.

Shine, K.P. 1984. Parameterization of shortwave flux over high albedo surfaces as function of cloud thickness and surface albedo. *Quarterly Journal of the Royal Meteorological Society*, **110**, 747–760.

Simonsen, K. & Haugan, P.M. 1996. Heat budgets of the Arctic Mediterranean and sea surface heat flux parameterizations for the Nordic Seas. *Journal of Geophysical Research*, **101**, 6553–6576.

Trenberth, K.E. & Olson, J.G. 1988. Evaluation and intercomparison of global analyses from the National Meteorological Center and the European Centre for Medium Range Weather Forecasts. *Bulletin of the American Meteorological Society*, **69**, 1047–1057.

Trumbore, S.E., Jacobs, S.S. & Smethie Jr, W.M. 1991. Chlorofluorocarbon evidence for rapid ventilation of the Ross Sea. *Deep-Sea Research*, **38**, 845–870.

Van Woert, M.L. 1999. Wintertime dynamics of the Terra Nova Bay polynya. *Journal of Geophysical Research*, **104**(C4), 7753–7769.

Zillman, J.W. 1972. *A study of some aspects of the radiation and the budgets of the Southern Hemisphere Oceans. Meteorological Study* No. 26. Canberra: Bureau of Meteorology, 562 pp.